Modelling Simul. Mater. Sci. Eng. **4** (1996) 349–357. Printed in the UK

Material parameters of quaternary III–V semiconductors for multilayer mirrors at 1.55 μm wavelength

M Guden† and J Piprek

University of Delaware, Materials Science Program, Newark, DE 19716, USA

Received 3 January 1996, accepted for publication 24 April 1996

Abstract. Nine quaternary (Al,Ga,In)–(P,As,Sb) semiconductor compounds lattice matched to InP are investigated theoretically. Direct bandgap, refractive index at 1.55 μm wavelength, and thermal conductivity are calculated as a function of the composition. These material properties are important, e.g. in distributed Bragg reflectors of vertical-cavity lasers. The alloy systems AlGaAsSb, AlGaPSb and GaInPSb are found to promise better performance of those mirrors than the common InGaAsP system.

1. Introduction

Semiconductors that are composed out of elements from the third group (Al,Ga,In) and the fifth group (P, As, Sb) of the periodic system are key materials for optoelectronic devices. Those compounds exhibit the zinc-blende type crystal lattice and a variety of materials can be achieved by mixing elements of the same group within the lattice. Most common is $Ga_xIn_{1-x}P_yAs_{1-y}$ ($x = 0, \ldots, 1$, $y = 0, \ldots, 1$) whose material properties have been widely investigated [1]. The compositional plane (x, y) of those quaternaries includes four binary alloys (for x and $y = 0$ or 1) and four ternary alloys (for x or $y = 0$ or 1). In general, material properties vary considerably with composition (x, y) and interpolation schemes have been developed using measured data of binary and ternary compounds.

The variety of material properties accessible with III–V semiconductor compounds can be employed in the design of advanced optoelectronic devices. A key component of some of those devices are highly reflective stacks of two alternating materials having different refractive indices and low absorption. If each layer thickness equals a quarter of the light wavelength, the Bragg condition of maximum reflectivity is fulfilled. Such distributed Bragg reflectors (DBRs) can exhibit more than 99% reflectivity. DBRs are utilized, e.g., in vertical-cavity surface-emitting lasers (VCSELs) [2]. Those mirrors are required to combine several important physical properties: high difference in the refractive index of the two layers, low absorption, and high thermal conductivity to minimize laser heating. In our case of semiconductor DBRs, high electrical conductivity that is restricted in the perpendicular direction by the difference of the electron bandgaps of both materials is also desirable. This problem can be solved by compositional grading or by suitable doping profiles at the interfaces [3].

Currently, some efforts are directed towards employing a wider range of III–V semiconductor alloys within DBRs. A target light wavelength is 1.55 μm that is used

† Also at Institute of Technology, Izmir, 35230, Turkey.

0965-0393/96/040349+09$19.50 © 1996 IOP Publishing Ltd

for long distance optical communication. The operation of 1.55 μm VCSELs using GaInPAs/InP DBRs is restricted to low temperatures and alternative DBR materials are highly desirable [4]. In the present paper, we investigate the whole compositional range of quaternary (Al,Ga,In)–(P,As,Sb) compounds that are lattice matched to InP, which is the most common substrate material for 1.55 μm devices. Table 1 gives the lattice match condition $y(x)$ for alloys under consideration. We focus on three key properties of these compounds to find suitable compositions for DBR mirrors: the direct bandgap E_0, the refractive index n at 1.55 μm wavelength, and the thermal conductivity k.

Table 1. Lattice match conditions $y(x)$ of III–V compounds to InP.

No	Alloy	Matching condition y
1	$Al_xGa_{1-x}P_ySb_{1-y}$	$(0.227 + 0.040x)/(0.645 + 0.040x)$
2	$Al_xGa_{1-x}As_ySb_{1-y}$	$(0.227 + 0.040x)/(0.443 + 0.033x)$
3	$Al_xGa_yIn_{1-x-y}As$	$(0.189 + 0.398x)/0.405$
4	$Al_xIn_{1-x}P_yAs_{1-y}$	$(0.189 - 0.398x)/(0.189 + 0.020x)$
5	$Al_xIn_{1-x}P_ySb_{1-y}$	$(0.610 - 0.343x)/(0.610 + 0.075x)$
6	$Al_xIn_{1-x}As_ySb_{1-y}$	$(0.610 - 0.343x)/(0.421 + 0.055x)$
7	$AlP_xAs_ySb_{1-x-y}$	$(0.267 - 0.685x)/0.058$
8	$Ga_xIn_{1-x}P_yAs_{1-y}$	$(0.189 - 0.405x)/(0.189 + 0.013x)$
9	$Ga_xIn_{1-x}P_ySb_{1-y}$	$(0.610 - 0.383x)/(0.610 + 0.035x)$
10	$Ga_xIn_{1-x}As_ySb_{1-y}$	$(0.610 - 0.383x)/(0.421 + 0.022x)$
11	$GaP_xAs_ySb_{1-x-y}$	$(0.227 - 0.645x)/0.443$

2. Theoretical models

Because of the random distribution of elements from the same group within the alloy lattice, exact calculations of material parameters are hardly possible. Instead, material data of quaternary alloys (Q) are predicted by interpolating known binary (B) or ternary (T) alloy data. Linear interpolation

$$Q^a_{\text{lin}}(x, y) = xyB_{AC} + x(1-y)B_{AD} + (1-x)yB_{BC} + (1-x)(1-y)B_{BD} \tag{1a}$$

for compounds $A_xB_{1-x}C_yD_{1-y}$ or

$$Q^b_{\text{lin}}(x, y) = xB_{AB} + yB_{AC} + (1-x-y)B_{AD} \tag{1b}$$

for compounds $AB_xC_yD_{1-x-y}$ is well established for calculating the lattice constant (Vegard's law) and equations (1) are used to determine the lattice matching conditions given in table 1.

For the thermal resistivity $W = k^{-1}$, the approximate interpolation scheme [5] includes bowing contributions Q_{bow} that are added to the corresponding linear formulae Q_{lin} in equations (1),

$$Q^a_{\text{bow}}(x, y) = -x(1-x)\left[yC_{ABC} + (1-y)C_{ABD}\right] - y(1-y)\left[xC_{ACD} + (1-x)C_{BCD}\right] \tag{2a}$$

$$Q^b_{\text{bow}}(x, y) = -xyC_{ABC} - x(1-x-y)C_{ABD} - y(1-x-y)C_{ACD} \tag{2b}$$

employing bowing parameters C that are obtained for ternary compounds

$$T_{ABC}(x) = xB_{AB} + (1-x)B_{AC} + x(x-1)C_{ABC}. \tag{3}$$

In our paper, the bowing parameter C is negative, if alloying causes larger values Q or T than observed in binary materials (B). All binary and bowing parameters used in our calculations are listed in section 3.

In the case of the direct bandgap E_0 and the spin-orbit valence band splitting Δ_0 (required to calculate the refractive index), the interpolation formulae are usually written as [6]

$$Q^a(x,y) = [x(1-x)[yT_{ABC}(x) + (1-y)T_{ABD}(x)] + y(1-y)[xT_{ACD}(y) + (1-x)T_{BCD}(y)]][x(1-x) + y(1-y)]^{-1} \quad (4a)$$

$$Q^b(x,y) = \frac{xyT_{ABC}(u) + y(1-x-y)T_{ACD}(v) + x(1-x-y)T_{ABD}(w)}{xy + y(1-x-y) + x(1-x-y)} \quad (4b)$$

with

$$u = (1-x+y)/2 \qquad v = (2-x-2y)/2 \qquad w = (2-2x-y)/2$$

(equation (18a) of [6] has been corrected). The direct bandgap E_0 should not be smaller than the photon energy of 0.8 eV to avoid strong absorption.

The refractive index of quaternary materials for photon energies $\hbar\omega$ below the direct bandgap E_0 can be expressed by [1]

$$n = \sqrt{A\left[f(x_0) + 0.5\left(\frac{E_0}{E_0+\Delta_0}\right)^{1.5} f(x_{os})\right] + B} \quad (5)$$

with

$$f(x_0) = x_0^{-2}\left(2 - \sqrt{1+x_0} - \sqrt{1-x_0}\right)$$

$$f(x_{os}) = x_{os}^{-2}\left(2 - \sqrt{1+x_{os}} - \sqrt{1-x_{os}}\right)$$

$$x_0 = \hbar\omega/E_0 \qquad x_{os} = \hbar\omega/(E_0+\Delta_0)$$

(equations (8.23a) and (8.23b) of [1] have been corrected). The material parameters A and B are linear interpolations of binary data obtained from measurements, A gives the strength of the E_0 and $E_0+\Delta_0$ transitions and B takes into account non-dispersive contributions from higher-energy transitions. Equation (5) is known to slightly overestimate the refractive index for photon energies close to E_0, but the investigated E_0 range will be restricted anyway to ensure low absorption (see below). With higher p-doping, intervalence band transitions might occur at 1.55 μm and may cause deviations from the calculated values.

It should be noted that equations (1) and (2) give the same results as equations (4) only for ternary (or binary) endpoints of the compositional range of each quaternary compound. Equations (4) seem to be more appropriate when using bowing parameters C obtained for ternary compounds. However applying equations (4) to the thermal resistance W delivers quaternary data that are maximum for ternary endpoints of quaternary compositions, in disagreement with experimental observations.

3. Material parameters

Table 2 summarizes all binary material parameters used. Binary lattice constants and energy data are obtained from [7]. Refractive index parameters A and B are given in [6] and [8], except the values of AlP that have been extrapolated. Thermal conductivities are published in [5], only the value of AlP is taken from [9].

Table 3 displays all ternary bowing parameters that are employed in our calculations. Energy bowing parameters of most ternary alloys of interest are found in [7]. For AlPSb and GaPSb, $C(E_0)$ is fitted to measurements [10] and $C(\Delta_0)$ is interpolated. The bowing

Table 2. Binary material data used in the calculations (a, lattice constant; E_0, direct bandgap; Δ_0, spin-orbit splitting; A, B, refractive index parameters in equation (5); k, thermal conductivity).

Binary	a (Å)	E_0 (eV)	Δ_0 (eV)	A	B	κ (W cm^{-1} K^{-1})
AlP	5.451	3.58	0.07	24.10	−2.00	1.30
AlAs	5.660	2.95	0.28	25.30	−0.80	0.91
AlSb	6.136	2.22	0.65	59.68	−9.53	0.57
GaP	5.451	2.74	0.08	22.25	0.90	0.77
GaAs	5.653	1.42	0.34	6.30	9.40	0.44
GaSb	6.096	0.72	0.82	4.05	12.66	0.33
InP	5.869	1.35	0.11	8.40	6.60	0.68
InAs	6.058	0.36	0.38	5.14	10.15	0.27
InSb	6.479	0.17	0.81	7.91	13.07	0.17

Table 3. Bowing parameters C of ternary compounds as used in the calculations ($*$, $C(W)$ data from measurements).

Alloy	$C(E_0)$	$C(\Delta_0)$	$C(W)$
Al(As,Sb)	0.840	0.15	−65.0
Al(P,Sb)	3.560	0.00	−101.0
Al(P,As)	0.00	0.00	−39.0
Ga(As,Sb)	1.200	0.60	−63.0
Ga(P,Sb)	2.558	0.00	−91.0
Ga(P,As)	0.210	0.00	−21.6*
In(As,Sb)	0.580	1.20	−80.0
In(P,Sb)	1.300	0.75	−115.0
In(P,As)	0.280	0.10	−34.0
(Al,Ga)P	0.000	0.00	−30.0
(Al,ln)P	0.000	0.00	−77.0
(Ga,In)P	0.790	0.00	−19.9*
(Al,Ga)As	0.370	0.00	−30.0*
(Al,ln)As	0.700	0.15	−80.0
(Ga,ln)As	0.380	0.15	−78.8*
(Al,Ga)Sb	0.470	0.30	−34.0*
(Al,ln)Sb	0.000	0.00	−88.0
(Ga,ln)Sb	0.420	0.00	−68.0

parameter of the thermal resistivity $C(W)$ has been measured for few ternary compounds only (marked with $*$) [5]. All other values of $C(W)$ are obtained by fitting equation (3) to results of the theoretical model of [11], further measurements are recommended for verification.

4. Results

For the eleven compounds of table 1, the direct bandgap E_0(x) has been calculated and it is larger than the target photon energy of 0.8 eV in most cases. As soon as E_0 approaches 0.8 eV, interband absorption occurs which strongly reduces the DBR reflectivity. To prevent this absorption, a minimum 'allowed' energy $E_0(x)$ of 0.9 eV is assumed that considers wavelength deviations as well as bandgap narrowing effects. This condition restricts the compositional range investigated and it excludes (10) GaInAsSb and (11) GaPAsSb of

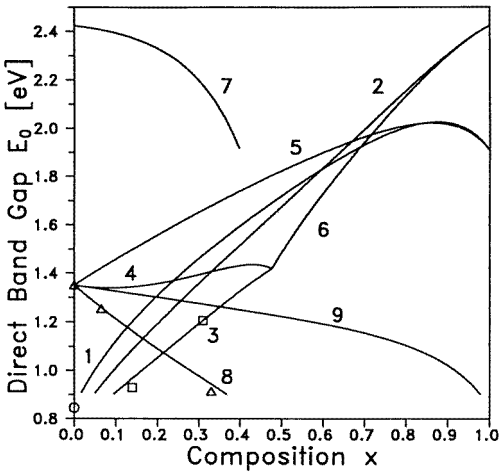

Figure 1. Calculated direct bandgap E_0 as a function of the composition x for quaternary III–V compounds lattice matched to InP (using numbering in tables 1 and 4). Measured data of (3) AlGaInAs □ [12], (8) GaInPAs △ [13] and (1) AlGaPSb ○ [22] are given for comparison.

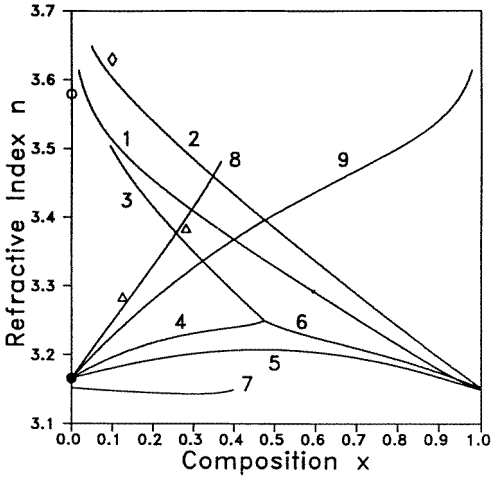

Figure 2. Calculated refractive index values at 1.55 μm wavelength as a function of the composition x (using numbering in tables 1 and 4). Measured data of (8) GaInPAs △ [14, 15], (1) AlGaPSb ○ [22], (2) AlGaAsSb ◊ [21] and InP • [16] are given for comparison.

table 1 from further consideration (the numbering in tables 1 and 4 is used to identify the corresponding quaternary alloy). The resulting direct bandgaps $E_0(x)$ are displayed in figure 1 for the remaining nine compounds. It should be mentioned that some of these alloys are indirect semiconductors, but the transition cannot be clearly marked due to insufficient data for the indirect bandgap. In figure 1, measured bandgap energies show good agreement.

Figure 2 depicts the calculated refractive index values at 1.55 μm wavelength. For the purpose of comparison, a few available experimental refractive index values are indicated and they are close to the calculated results.

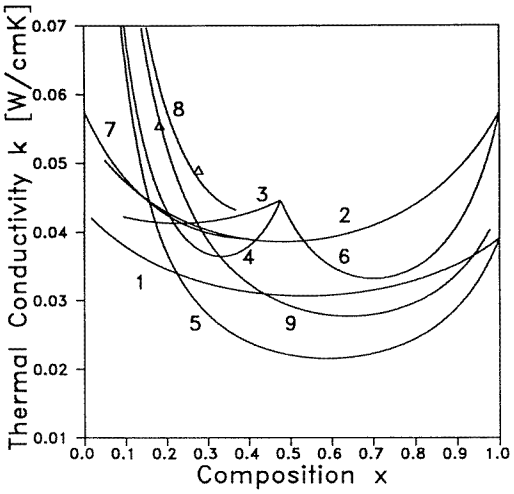

Figure 3. Calculated thermal conductivity as function of the composition x (using numbering in tables 1 and 4). Measured data of (8) GaInPAs △ [17] are given for comparison.

For the III–V compounds of interest, the resulting thermal conductivities are plotted in figure 3 in the range of low values. Only those compositions close to the binary InP exhibit a strong increase of k towards the InP value of 0.68 W cm^{-1} K^{-1} (not shown). Ternary and quaternary alloys are known to exhibit very small thermal conductivities due to disorder scattering of phonons. Towards the endpoints of the compositional ranges, less alloying elements are present, resulting in higher thermal conductivities. Measured data of quaternaries are only available for (8) GaInAsP [17] and show good agreement with the interpolation.

5. Discussion

Table 4 summarizes the results at the endpoints of the investigated compositional range for each compound. Large refractive index differences are the first criterion in selecting materials for DBRs. According to table 4, the strongest variation within one compound occurs for (2) AlGaAsSb ($\Delta n = 0.50$), followed by (1) AlGaPSb ($\Delta n = 0.46$) and (9) GaInPSb ($\Delta n = 0.44$). The common alloy (8) GaInPAs shows a variation of $\Delta n = 0.31$ in agreement with measured data [18]. In all these cases, larger differences seem to be possible with $E_0(x) < 0.9$ eV, approaching one of the three ternary compounds that exhibit high refractive indices: (2) GaAsSb, (1,9) GaPSb or (8) GaInAs. However, all three ternaries have direct bandgaps close to or even below the photon energy of 0.8 eV, hence strong band-to-band transitions would limit the reflectivity. In table 5, experimental results on 1.55 μm DBRs are compared to the calculated power reflectance R_{cal} [19] of lossless quarter-wavelength multilayer stacks using refractive index values of our analysis. Such comparison is difficult since real DBRs can be expected to exhibit some absorption as well as some deviation from ideal layer thicknesses. The examples of table 5 are discussed in the following. (1) GaPSb/AlPSb DBRs [10] reach 99% reflectance using only 20 pairs of mirror layers. The agreements with our estimation is quite good since the bandgap of AlPSb is still above the photon energy. Measurements on (2) AlGaAsSb DBRs [20, 21] show high reflectances in good agreement with our calculations as far as ternary alloys with

Table 4. Endpoint data from graphs in figures 1–3.

No	Alloy	x	y	E_0	n	κ
1	AlGaPSb	0.02	0.35	0.91	3.61	0.046
		1.00	0.40	1.91	3.15	0.039
2	AlGaAsSb	0.05	0.52	0.91	3.65	0.062
		1.00	0.56	2.42	3.15	0.057
3	AlGalnAs	0.09	0.37	0.90	3.50	0.050
		0.47	0.00	1.42	3.25	0.045
4	AllnPAs	0.00	1.00	1.35	3.17	0.680
		0.47	0.00	1.42	3.25	0.044
5	AllnPSb	0.00	1.00	1.35	3.17	0.680
		0.47	0.00	1.42	3.25	0.045
6	AllnAsSb	0.48	1.00	1.42	3.25	0.045
		1.00	0.56	2.42	3.15	0.057
7	AlPAsSb	0.00	0.56	2.42	3.15	0.057
		0.40	0.00	1.92	3.15	0.039
8	GalnPAs	0.00	1.00	1.35	3.17	0.680
		0.36	0.21	0.90	3.48	0.072
9	GalnPSb	0.00	1.00	1.35	3.17	0.680
		0.98	0.37	0.90	3.61	0.046

Table 5. Comparison of experimental and calculated DBR mirror reflectances $R(E_0^{\min}$, minimum direct bandgap).

No	DBR Alloys	No of pairs	$R_{\exp}$(%)	R_{cal}(%)	$E_0^{\min}$(eV)
1	$GaP_{0.35}Sb_{0.65}/AlP_{0.4}Sb_{0.6}$	20	99.0	99.8	0.85
2	$GaAs_{0.51}Sb_{0.49}/AlAs_{0.56}Sb_{0.44}$	$8\frac{1}{2}$	~ 80	94.3	0.78
2	$Al_{0.1}Ga_{0.9}As_{0.518}Sb_{0.482}/AlAs_{0.56}Sb_{0.44}$	$15\frac{1}{2}$	95.3	97.9	1.01
8	$Ga_{0.47}In_{0.53}As/InP$	20	98.0	99.7	0.75
8	$Ga_{0.37}In_{0.63}P_{0.202}As_{0.798}/InP$	45	99.9	99.9	0.90
		20	92.5	97.5	0.90
		10	80.0	84.2	0.90

low bandgaps are omitted. Bandgaps E_0 below the photon energy 0.8 eV cause a strong reduction of the DBR reflectivity due to interband absorption that is not included in our calculation (see second row in table 5). Interband absorption at photon energies near the bandgap can be reduced by high n-doping [23]. This Burstein effect has been used in (8) InGaAs/InP DBRs [25] employing n-doped InGaAs with a calculated bandgap of 0.75 eV, but at very high n-doping levels, free carrier absorption may dominate and hence limit the reflectivity. The effect of p-doping on the absorption is the reverse of that of n-doping: it tends to increase near band-edge absorption due to the impurity bands which form at the acceptor level [24]. For comparison, some results with the common DBR alloy system (8) GaInPAs/InP are listed at the end of table 5 [26]. Because of the low refractive index difference, large numbers of mirror pairs are required to obtain reflectances above 99%. Those thick DBRs are difficult to manufacture.

No measurements on (9) GaInPSb DBRs, the third material system with high Δn, have been found so far. GaPSb/InP DBRs would not only have a high refractive index difference, but also a relatively high lateral thermal conductivity because of the binary InP layer

involved. DBRs of AlGaAsSb and AlGaPSb without a binary layer are expected to exhibit very low thermal conductivities (see figure 3). Combinations of high index compositions (low x) of both quaternary systems with InP would hardly reduce the reflectivity but increase the thermal conductivity, but interdiffusion of specific elements within those combinations might limit the DBR performance.

6. Summary

The direct bandgap, the refractive index at 1.55 μm, and the thermal conductivity of (Al,Ga,In)–(P,As,Sb) quaternary compounds on InP are calculated using interpolation schemes. The compositional range of those compounds has been restricted to allow only bandgaps above 0.9 eV and to avoid considerable absorption at 1.55 μm wavelength. Largest variations of the refractive index are found within the systems AlGaAsSb ($\Delta n = 0.50$), AlGaPSb ($\Delta n = 0.46$), and GaInPSb ($\Delta n = 0.44$) that promise higher reflectivities of thin DBR mirrors than the common GaInPAs system ($\Delta n = 0.31$). The thermal conductivity of most quaternary and ternary compounds is calculated to be very low (0.02–0.06 W cm^{-1} K^{-1}), except for those compositions that are close to InP (0.68 W cm^{-1} K^{-1}). It seems to be advantageous to combine high index compositions of the above-mentioned alloys with InP to achieve mirrors with higher lateral thermal conductivity. Besides those compounds that have already been investigated experimentally, GaInPSb is identified as a new target material for DBRs at 1.55 μm wavelength.

References

[1] Adachi S 1992 *Physical Properties of III–V Semiconductor Compounds* (New York: Wiley)

[2] Agrawal G P (ed) 1995 *Semiconductor Lasers* (Woodbury: AIP)

[3] Peters M G, Thibeault B J, Young D B, Gossard A C and Coldren L A 1994 Growth of beryllium doped $Al_xGa_{1-x}As$/GaAs mirrors for vertical-cavity surface-emitting lasers *J. Vac. Sci. Technol.* B **12** 3075–83

[4] Piprek J, Wenzel H, Braun D, Wünsche H -J, and Henneberger F 1995 Modeling light vs current characteristics of long-wavelength vertical-cavity surface-emitting laser diodes with various distributed Bragg reflector materials *SPIE vol 2399: Physics and Simulation of Optoelectronic Devices III* ed M A Osinski and W W Chow pp 605–16

[5] Nakwaski W 1988 Thermal conductivity of binary, ternary, and quaternary III–V compounds *J. Appl. Phys.* **64** 159–66

[6] Adachi S 1987 Band gaps and refractive indices of AlGaAsSb, GaInAsSb, and InPAsSb: Key properties for a variety of the 2–4 μm optoelectronic device applications *J. Appl. Phys.* **61** 4869–76

[7] Krijn M P C M 1991 Heterojunction band offsets and effective masses in III–V quaternary alloys *Semicond. Sci. Technol.* **6** 27–31

[8] Adachi S 1982 Refractive indices of III–V compounds: Key properties of InGaAsP relevant to device design *J. Appl. Phys.* **53** 5863–9

[9] Bhandari C M and Rowe D M 1988 *Thermal Conduction in Semiconductors* (New York: Wiley)

[10] Anan T, Shimomura H and Sugou S 1994 Improved reflectivity of AlPSb/GaPSb Bragg reflector for 1.55 μm wavelength *Electron. Lett.* **30** 2138–9

[11] Abeles B 1963 Lattice thermal conductivity of disordered semiconductor alloys at high temperatures *Phys. Rev.* **131** 1906–11

[12] Olego D, Chang T Y, Silberg E, Caridi E A and Pinczuk A 1982 Compositional dependence of band-gap energy and conduction-band effective mass of $In_{1-x-y}Ga_x$ Al_yAs lattice matched to InP *Appl. Phys. Lett.* **41** 476–8

[13] Nakajima K, Yamaguchi A, Akita K and Kotani T 1978 Composition dependence of the bandgaps of $In_{1-x}Ga_xAs_{1-y}P_y$ quaternary solids lattice matched on InP substrates *J. Appl. Phys.* **49** 5944–50

[14] Chandra P, Coldren L A and Strege K E 1981 Refracrive Index data from $Ga_xIn_{1-x}As_yP_{1-y}$ films *Electron. Lett.* **17** 6–7

[15] Tai K, McColl S L and Chu S N G 1987 Chemicalbeam epitaxially grown InP/InGaAsP interference mirror for use near 1.55 μm wavelength *Appl. Phys. Lett.* **51** 826–7
[16] Petit G D and Turner W J 1965 Refractive index of InP *J. Appl. Phys.* **36** 2081
[17] Both W, Gottschalch V and Wagner G 1986 Thermal resistivity of GaInAsP alloy. Experimental Results *Cryst. Res. Technol.* **21** K85–K87
[18] K Streubel, Royal Institute of Technology, Stockholm, Sweden, unpublished
[19] Corzine S W, Yan R H and Coldren L A 1991 A tanh substitution technique for the analysis of abrupt and graded interface multilayer dielectric stacks *Quant. Electron. Lett.* **27** 2086–90
[20] Blum O, Fritz I J, Dawson L R, Howard A J, Headley T J, Olsen J A, Klem J F and Drummond T J 1994 Molecular beam epitaxy AlAsSb/GaAsSb distributed Bragg reflector on InP substrate operating near 1.55 μm *J. Vac. Sci. Technol.* B **12** 1122–4
[21] Blum O, Fritz I J, Dawson L R and Drummond T J 1995 Digital alloy AlAsSb/AlGaAsSb distributed Bragg reflectors lattice matched to InP for 1.3–1.55 μm wavelength range *Electron. Lett.* **31** 1247–8
[22] Shimomura H, Anan T, Mori K and Sugou S 1994 High-reflectance AlPSb/GaPSb distributed Bragg reflector mirrors on InP grown by gas-source molecular beam epitaxy *Electron. Lett.* **30** 314–5
[23] Burstein E 1954 Anomalous optical absorption limit in InSb *Phys. Rev.* **93** 632–3
[24] Deppe D G, Gerrerd N D, Pinzone C J, Dupuis R D and Schubert E F 1990 Quarter-wave Bragg reflector stack on InP-$In_{053}Ga_{047}As$ *Appl. Phys. Lett.* **56** 315–17
[25] Guy P, Woodbridge K, Haywood S K and Hopkinson M 1994 Highly doped 1.55 μm $Ga_xIn_{1-x}As$/InP distributed Bragg reflector stack *Electron. Lett.* **30** 1526–7
[26] Choa F S, Tai K, Tsang W T and Chu S N G 1991 High reflectivity 1.55 μm InP/InGaAsP Bragg mirror grown by chemical beam epitaxy *Appl. Phys. Lett.* **59** 2820–2